

Cite this: *Chem. Sci.*, 2017, **8**, 5797

## Efficient photocatalytic carbon monoxide production from ammonia and carbon dioxide by the aid of artificial photosynthesis†

Zeai Huang, <sup>a</sup> Kentaro Teramura, <sup>ab</sup> Hiroyuki Asakura, <sup>ab</sup> Saburo Hosokawa <sup>ab</sup> and Tsunehiro Tanaka <sup>ab</sup>

Ammonium bicarbonate ( $\text{NH}_4\text{HCO}_3$ ) was generated by the absorption of carbon dioxide ( $\text{CO}_2$ ) into an aqueous solution of ammonia ( $\text{NH}_3$ ).  $\text{NH}_4\text{HCO}_3$  was successfully used to achieve highly efficient photocatalytic conversion of  $\text{CO}_2$  to carbon monoxide (CO).  $\text{NH}_3$  and/or ammonium ions ( $\text{NH}_4^+$ ) derived from  $\text{NH}_4\text{HCO}_3$  in aqueous solution were decomposed into nitrogen ( $\text{N}_2$ ) and hydrogen ( $\text{H}_2$ ). Stoichiometric amounts of the  $\text{N}_2$  oxidation product and the CO and  $\text{H}_2$  reduction products were generated when the photocatalytic reaction was carried out in aqueous  $\text{NH}_4\text{HCO}_3$  solution.  $\text{NH}_3$  and/or  $\text{NH}_4^+$  functioned as electron donors in the photocatalytic conversion of  $\text{CO}_2$  to CO. A CO formation rate of  $0.5 \text{ mmol h}^{-1}$  was obtained using  $500 \text{ mg}$  of catalyst (approximately  $7500 \text{ ppm}$ ) in ambient conditions ( $303 \text{ K}$ ,  $101.3 \text{ kPa}$ ). Our results demonstrated that  $\text{NH}_4\text{HCO}_3$  is a novel inorganic sacrificial reagent, which can be used to increase the efficiency of photocatalytic CO production to achieve one step  $\text{CO}_2$  capture, storage and conversion.

Received 26th April 2017  
Accepted 19th June 2017

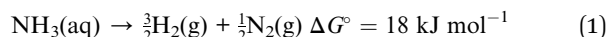
DOI: 10.1039/c7sc01851g  
[rsc.li/chemical-science](http://rsc.li/chemical-science)

## Introduction

The production of chemical feedstocks and hydrocarbon fuels from  $\text{CO}_2$  is a promising approach to alleviate the global energy crisis and global warming.<sup>1</sup> Conversion of  $\text{CO}_2$  to CO using clean and renewable solar energy is the first step to store energy in chemicals because CO can be further converted into other highly valuable chemicals using the Fischer–Tropsch process.<sup>2</sup> A variety of heterogeneous and homogeneous photocatalysts have been reported to achieve the conversion of  $\text{CO}_2$  to CO.<sup>3–5</sup> However, the formation rate of CO has been limited to a few tens of  $\mu\text{mol h}^{-1}$  or hundreds of  $\mu\text{mol h}^{-1} \text{ g}^{-1}$  because of the high energy barrier to  $\text{CO}_2$  reduction and inefficient light utilization.<sup>6,7</sup> Furthermore,  $\text{CO}_2$  is not easily adsorbed onto catalytic surfaces nor activated by photoirradiation because of its high thermodynamic stability. This further reduces the efficiency of the photocatalytic conversion of  $\text{CO}_2$ .

Water ( $\text{H}_2\text{O}$ ) is widely used as an electron donor in the photocatalytic conversion of  $\text{CO}_2$  to CO.<sup>7–12</sup> However, the overall water splitting into  $\text{H}_2$  and  $\text{O}_2$  is more thermodynamically favorable than the reduction of  $\text{CO}_2$  in aqueous solution. Hence,

$\text{CO}_2$  reduction competes with overall water splitting. Moreover, the solubility of  $\text{CO}_2$  in pure  $\text{H}_2\text{O}$  is only  $0.033 \text{ mol L}^{-1}$  (at  $298 \text{ K}$  and  $101.3 \text{ kPa}$ ),<sup>13</sup> which further limits the efficiency of  $\text{CO}_2$  conversion by  $\text{H}_2\text{O}$  using heterogeneous photocatalysts. Therefore, it would be meaningful to find a readily available, highly efficient, and abundant in nature and industries electron donor (sacrificial reagent) other than water for the photocatalytic conversion of  $\text{CO}_2$ .  $\text{NH}_3$  and  $\text{NH}_4^+$  in aqueous solution can be readily oxidized to  $\text{N}_2$ ,  $\text{NO}_2^-$ , and  $\text{NO}_3^-$  using a photocatalyst.<sup>14–17</sup> The decomposition of aqueous  $\text{NH}_3$  to  $\text{H}_2$  and  $\text{N}_2$  requires a standard Gibbs free energy change  $\Delta G^\circ$  of  $18 \text{ kJ mol}^{-1}$  (eqn (1)).<sup>18</sup> This is significantly smaller than that required for the decomposition of  $\text{H}_2\text{O}$  to  $\text{H}_2$  and  $\text{O}_2$  ( $237 \text{ kJ mol}^{-1}$ ; eqn (2)).



Because the photocatalytic oxidation of  $\text{NH}_3$  and  $\text{NH}_4^+$  is significantly more favorable than the oxidation of  $\text{H}_2\text{O}$  to  $\text{O}_2$ ,<sup>18</sup> it is possible to use  $\text{NH}_3$  and  $\text{NH}_4^+$  as electron donors in the photocatalytic conversion of  $\text{CO}_2$ . Moreover,  $\text{NH}_3$  has been considered for use as an efficient post-combustion  $\text{CO}_2$  capture and storage (CCS) reagent because of its high absorption efficiency and loading capacity.<sup>19</sup> The absorption and capture of  $\text{CO}_2$  by an aqueous solution of  $\text{NH}_3$  results in the formation of  $\text{NH}_4\text{HCO}_3$ .<sup>20</sup> Other basic species, such as  $\text{NaHCO}_3$  and  $\text{KHCO}_3$ , have been used to increase the solubility of  $\text{CO}_2$  in aqueous

<sup>a</sup>Department of Molecular Engineering, Graduate School of Engineering, Kyoto University, Kyoto 615-8510, Japan. E-mail: [teramura@moleng.kyoto-u.ac.jp](mailto:teramura@moleng.kyoto-u.ac.jp); [tanakat@moleng.kyoto-u.ac.jp](mailto:tanakat@moleng.kyoto-u.ac.jp)

<sup>b</sup>Elements Strategy Initiative for Catalysts and Batteries, Kyoto University, Kyoto 615-8510, Japan

† Electronic supplementary information (ESI) available: Experimental details, calculations and characterizations. See DOI: [10.1039/c7sc01851g](https://doi.org/10.1039/c7sc01851g)



solutions.<sup>21,22</sup> Previous reports have suggested that dissolved  $\text{CO}_2$ , rather than bicarbonate ( $\text{HCO}_3^-$ ) or carbonate ( $\text{CO}_3^{2-}$ ) ions, is the active species in the reduction of  $\text{CO}_2$ .<sup>23,24</sup> Correspondingly, the conversion of  $\text{CO}_2$  and/or the selectivity toward CO evolution have been significantly enhanced by the presence of bases in both photocatalytic (PC) and photoelectrochemical (PEC) cell systems.<sup>25,26</sup> In the present study, we designed the use of  $\text{NH}_4\text{HCO}_3$  for the efficient photocatalytic conversion of  $\text{CO}_2$  to CO in  $\text{H}_2\text{O}$ .

## Results and discussion

Flux-mediated crystal growth method shows the advantage of the synthetic control over particle sizes, morphologies, and surface features comparing with that of solid-state reaction method (SSR).<sup>27</sup> Modification of these features as a function of flux conditions have been reported to show significant enhancements in both water splitting and  $\text{CO}_2$  photoreduction.<sup>11,27,28</sup>  $\text{Sr}_2\text{KTa}_5\text{O}_{15}$  has been reported to show good activity and selectivity toward CO evolution when used as a photocatalyst in the conversion of  $\text{CO}_2$  by  $\text{H}_2\text{O}$  in our previous work.<sup>29</sup> In the present study,  $\text{Sr}_2\text{KTa}_5\text{O}_{15}$  was fabricated by a modified flux method, using a mixture of NaCl and KCl as the flux. The resultant catalyst was confirmed to have tetragonal tungsten bronze (TTB) structure (Fig. S1A†), and its real chemical formula was determined to be  $\text{Sr}_{1.6}\text{K}_{0.35}\text{Na}_{1.45}\text{Ta}_5\text{O}_{15}$  using ICP-OES. Its morphology was observed by SEM, and was found to consist of a mixture of nanorods and nanoparticles (Fig. S1B†).

Fig. 1 shows the time courses of the photocatalytic conversion of  $\text{CO}_2$  in  $\text{H}_2\text{O}$  and aqueous solutions of  $\text{NaHCO}_3$  and  $\text{NH}_4\text{HCO}_3$ . In pure  $\text{H}_2\text{O}$ , only 16.8  $\mu\text{mol}$  of CO was evolved after 5 h of photoirradiation (Fig. 1A), and the main reduction product was  $\text{H}_2$  (139.0  $\mu\text{mol}$ ). These results were consistent with previous reports.<sup>25,29</sup> In this system, overall water splitting proceeded more readily than  $\text{CO}_2$  reduction, resulting in the generation of  $\text{H}_2$  as the major product, rather than CO. The amount of CO evolved in 0.1 M aqueous  $\text{NaHCO}_3$  solution after 5 h of photoirradiation (448.7  $\mu\text{mol}$ ) was 26.7 times higher than that evolved in pure  $\text{H}_2\text{O}$  (Fig. 1B). However, the formation of  $\text{H}_2$  (94.7  $\mu\text{mol}$ ) was not significantly affected by  $\text{NaHCO}_3$ . Thus,

$\text{NaHCO}_3$  greatly enhanced the conversion of  $\text{CO}_2$  to CO without affecting the water splitting process.<sup>25</sup> In both pure  $\text{H}_2\text{O}$  and 0.1 M aqueous  $\text{NaHCO}_3$ , stoichiometric amounts of  $\text{O}_2$  were evolved continuously during the reaction, implying that  $\text{H}_2\text{O}$  functioned as an electron donor in the reduction of  $\text{CO}_2$ . Moreover, the evolution of CO increased dramatically in 0.1 M aqueous  $\text{NH}_4\text{HCO}_3$  solution; 1600  $\mu\text{mol}$  (1.6 mmol) of CO was evolved after 5 h of photoirradiation (Fig. 1C). This is 94.2 times greater than the amount evolved in pure  $\text{H}_2\text{O}$ . The selectivity of the reaction toward CO evolution was calculated and the details were shown in ESI.† The selectivity toward CO evolution in 0.1 M aqueous  $\text{NH}_4\text{HCO}_3$  (86.2%) was similar to that in aqueous  $\text{NaHCO}_3$  (82.5%). The production of gaseous products was negligible in blank tests conducted without either a catalyst or photoirradiation (Fig. S2A and B†). Thus, both are necessary for the photocatalytic conversion of  $\text{CO}_2$  to CO to proceed. Without Ag cocatalyst,  $\text{H}_2$  was formed as main product (Fig. S2C†), both of  $\text{N}_2$  and  $\text{O}_2$  were detected as oxidation products, however, the amount of these gases was far beyond the stoichiometric amount. Tiny amount of CO was formed after 5 hour photoirradiation (14.9  $\mu\text{mol}$ ). Ag cocatalysts were important in photocatalytic conversion of  $\text{CO}_2$  to CO, which is thought to be the active sites.  $\text{H}_2$ , CO, and  $\text{N}_2$  were obtained without a continuous  $\text{CO}_2$  flow (Fig. S2D†). However,  $\text{H}_2$  was generated as a major product, suggesting a very low selectivity toward CO evolution (less than 30%). This suggested that  $\text{CO}_2$  presence significantly increases the selectivity of the photocatalytic conversion of  $\text{CO}_2$  toward CO evolution in  $\text{NH}_4\text{HCO}_3$  solution.  $\text{NH}_4\text{HCO}_3$  can be formed directly by the absorption of  $\text{CO}_2$  in an aqueous solution of  $\text{NH}_3$ ; wherein  $\text{H}_2$  and CO can be produced from  $\text{CO}_2$  and  $\text{NH}_3$  via artificial photosynthesis. Thus, our designed system can achieve carbon capture and utilization (CCU) in a single process.

$\text{N}_2$ , rather than  $\text{O}_2$ , was generated as the oxidation product during photoirradiation in the presence of  $\text{NH}_4\text{HCO}_3$  (Fig. 1C). This demonstrated that  $\text{H}_2\text{O}$  did not function as an electron donor in this system. Instead,  $\text{NH}_3$  and/or  $\text{NH}_4^+$  functioned as electron donors, because the  $\Delta G^\circ$  of  $\text{NH}_3\text{(aq)}$  oxidation (18  $\text{kJ mol}^{-1}$ ) is significantly lower than that of water oxidation (237  $\text{kJ mol}^{-1}$ ). Analysis of the liquid phase showed that neither  $\text{NO}_2^-$

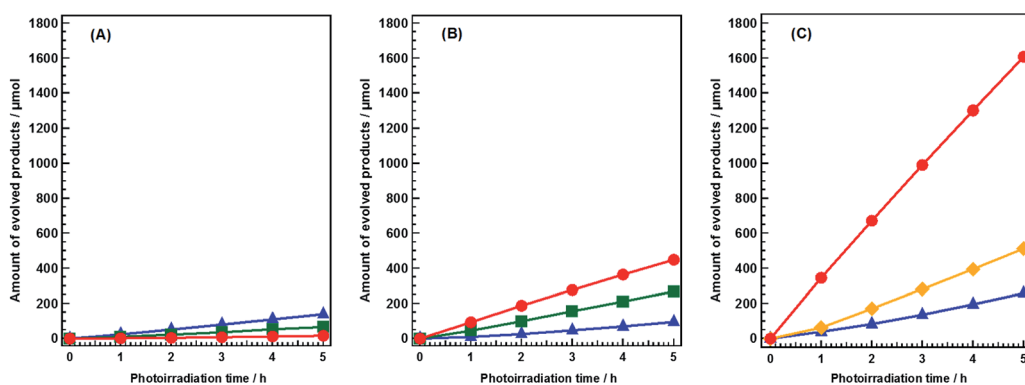


Fig. 1 Time courses of CO (circle),  $\text{O}_2$  (square),  $\text{N}_2$  (lozenge), and  $\text{H}_2$  (triangle) evolutions during the photocatalytic conversion of  $\text{CO}_2$  over Ag-modified  $\text{Sr}_{1.6}\text{K}_{0.35}\text{Na}_{1.45}\text{Ta}_5\text{O}_{15}$ . Amount of catalyst: 0.5 g; cocatalyst loading: 1.0 wt% Ag; light source: 400 W high-pressure Hg lamp; water volume: 1.0 L;  $\text{CO}_2$  flow rate: 30  $\text{mL min}^{-1}$ ; additive: (A) none, (B) 0.1 M  $\text{NaHCO}_3$ , or (C) 0.1 M  $\text{NH}_4\text{HCO}_3$ .



nor  $\text{NO}_3^-$  were present during photoirradiation (Fig. S3†). Other gaseous  $\text{NO}_x$  products, such as  $\text{N}_2\text{O}$  and  $\text{NO}$ , were not detected by gas chromatography (GC). These results indicated that  $\text{NH}_3$  and/or  $\text{NH}_4^+$  were oxidized only to  $\text{N}_2$  in this photocatalytic system. Hence, by using  $\text{NH}_4\text{HCO}_3$ , we succeeded in controlling the oxidation product, in addition to enhancing the conversion of  $\text{CO}_2$ .

The ratio of electrons to holes consumed in the photocatalytic conversion of  $\text{CO}_2$  was calculated to be 2.0 after 1 h of photoirradiation (Fig. S4†). Given that the total number of electrons generated must be the same as the number of holes, this ratio indicates that significantly more electrons were consumed than holes in the initial stages of photoirradiation. We noted that the state of Ag was changed from metallic to  $\text{Ag}^+$  on the surface of catalyst measured by XPS (Fig. S5†), however, it might be not the main reason for the excess of electron consumption. We calculated that if all  $\text{Ag}^0$  was changed to  $\text{Ag}^+$  in the first hour, the consumed holes were still only 469  $\mu\text{mol}$ , which was much less than the consumed electrons (770  $\mu\text{mol}$ ).  $\text{NH}_4^+$  can be reduced to  $\text{NH}_3$  and  ${}^{\cdot}\text{H}$  by photogenerated electrons. Hydrazine ( $\text{N}_2\text{H}_4$ ) has been determined to be an intermediate species in the photocatalytic decomposition of  $\text{NH}_3$  and/or  $\text{NH}_4^+$  to  $\text{H}_2$  and  $\text{N}_2$  using  $\text{Pt}/\text{TiO}_2$ .<sup>14</sup> Stoichiometric amounts of products, including  $\text{H}_2$  and  $\text{N}_2$ , were not obtained in the initial stages of photoirradiation due to the formation of hydrazine. In our system, it is also possible to form hydrazine at the beginning, however, hydrazine is reported to be reacted with  $\text{CO}_2$  to form zwitterionic intermediate and carbamate-type species,<sup>30</sup> which made the detection of intermediate oxidation species much more difficult. Nevertheless, stoichiometric amounts of products were obtained after 2 h of photoirradiation (Fig. S4†), indicating that the total decomposition of  $\text{NH}_3$  and/or  $\text{NH}_4^+$  occurred sooner.

The above results demonstrate that the highly efficient photocatalytic conversion of  $\text{CO}_2$  to CO was achieved in our system. The stoichiometric amounts of  $\text{H}_2$ ,  $\text{N}_2$  and CO generated indicated that  $\text{NH}_3$  and/or  $\text{NH}_4^+$  functioned as electron donors in the photocatalytic conversion of  $\text{CO}_2$ . Significantly greater photocatalytic activity was obtained using  $\text{NH}_3$  and/or  $\text{NH}_4^+$ , compared to reactions using  $\text{H}_2\text{O}$  as an electron donor under the same conditions.  $\text{NH}_3$  and/or  $\text{NH}_4^+$  are suitable for use in practical applications because  $\text{NH}_3$  is industrially produced in large quantities. Furthermore, in our photocatalytic system,  $\text{NH}_3$  and/or  $\text{NH}_4^+$  can be completely decomposed to  $\text{N}_2$ , which is an inert and non-toxic gas.

Table 1 shows the effects of  $\text{NH}_4\text{HCO}_3$  concentration on the photocatalytic conversion of  $\text{CO}_2$ . In pure  $\text{H}_2\text{O}$ , overall water splitting proceeded as the dominant reaction. Hence, the evolution of CO was negligible (entry 1). When the photocatalytic reaction was carried out in 0.01 M aqueous  $\text{NH}_4\text{HCO}_3$  the production of  $\text{H}_2$  resulting from water splitting was dramatically suppressed (entry 2). Because the oxidation of  $\text{NH}_3$  and/or  $\text{NH}_4^+$  to  $\text{N}_2$  proceeds more readily than the oxidation of  $\text{H}_2\text{O}$  to  $\text{O}_2$ , the formation rate of  $\text{O}_2$  in 0.01 M aqueous  $\text{NH}_4\text{HCO}_3$  was less than half that in pure  $\text{H}_2\text{O}$ . Even low concentrations of  $\text{NH}_4\text{HCO}_3$  (0.01 M) significantly increased the formation rate of CO, indicating that the presence of  $\text{NH}_4\text{HCO}_3$

is vital to achieving high photocatalytic activity.  $\text{NH}_4\text{HCO}_3$  can also be used to increase the pH of the reaction solution, to offset the decrease in pH caused by the dissolution of  $\text{CO}_2$ . With  $\text{CO}_2$  flowing, the pH of the reaction solution based on pure  $\text{H}_2\text{O}$  was 3.95, which increased to 5.88 with the addition of 0.01 M  $\text{NH}_4\text{HCO}_3$ . Increasing the pH also increases the amount of  $\text{CO}_2$  that can be dissolved in the reaction solution.<sup>31</sup> Generally, the formation rate of CO increases with increasing pH, because the reaction rate largely depends on the concentration of substrate. Therefore, the addition of  $\text{NH}_4\text{HCO}_3$  contributed to the efficient conversion of  $\text{CO}_2$  and the good selectivity toward CO evolution. Increasing the concentration of  $\text{NH}_4\text{HCO}_3$  from 0.01 M to 0.05 M completely suppressed the overall water splitting reaction, since only  $\text{N}_2$  was generated as an oxidation product (entry 3). The formation rate of CO increased with the concentration of  $\text{NH}_4\text{HCO}_3$ . Increasing the  $\text{NH}_4\text{HCO}_3$  concentration from 0.1 M to 1.0 M increased the formation rate of CO to 550.7  $\mu\text{mol h}^{-1}$  except the selectivity toward CO evolution decreased slightly, from 86.1% to 65.5% (entry 4 to 7). As previously discussed,  $\text{NH}_4\text{HCO}_3$  can be synthesized by flowing  $\text{CO}_2$  through an aqueous solution of  $\text{NH}_3$ . To determine whether  $\text{NH}_3$  functions as an electron donor under a flow of  $\text{CO}_2$ , we carried out the photocatalytic conversion of  $\text{CO}_2$  in an aqueous solution of  $\text{NH}_3$  (entry 8). The formation rate of CO was 547.2  $\mu\text{mol h}^{-1}$  in *ca.* 0.5 M aqueous  $\text{NH}_3$ , indicating that  $\text{NH}_3$  functions efficiently as an electron donor under these conditions. The ratio of photogenerated electrons to holes ( $e^-/\text{h}^+$ ) was estimated to be around 1.0 in reactions with high concentrations of aqueous  $\text{NH}_4\text{HCO}_3$  after 5 h of photoirradiation. This further supports the hypothesis that  $\text{NH}_3$  and/or  $\text{NH}_4^+$  function as effective electron donors during the photocatalytic conversion of  $\text{CO}_2$ .

To confirm that CO evolution originated from  $\text{CO}_2$  introduced in the gas phase, rather than from carbon contaminants, we conducted an isotopic labeling experiment. Fig. 2 shows mass spectra ( $m/z = 28$  and 29) obtained during the photocatalytic conversion of  ${}^{13}\text{CO}_2$  in 0.5 M aqueous  $\text{NH}_4\text{HCO}_3$  over Ag-

**Table 1** Photocatalytic conversion of  $\text{CO}_2$  over Ag-modified  $\text{Sr}_{1.6}\text{K}_{0.35}\text{Na}_{1.45}\text{Ta}_5\text{O}_{15}$  with different additive concentrations. Amount of catalyst: 0.5 g; cocatalyst loading: 1.0 wt% Ag; light source: 400 W high-pressure Hg lamp; water volume: 1.0 L;  $\text{CO}_2$  flow rate: 30 mL min $^{-1}$

Entry	$\text{NH}_4\text{HCO}_3^a/\text{M}$	Formation rate <sup>b</sup> / $\mu\text{mol h}^{-1}$				Selec. <sup>c</sup> (%)	$e^-/\text{h}^{+d}$
		$\text{H}_2$	$\text{O}_2$	$\text{N}_2$	CO		
1	0	35.9	16.3	Trace	3.6	9.2	1.21
2	0.01	16.9	7.0	12.3	54.5	76.3	1.17
3	0.05	23.8	Trace	42.3	146.7	86.1	1.34
4	0.1	48.4	Trace	94.3	270.4	84.8	1.13
5	0.5	119.8	Trace	193.6	512.9	81.1	1.09
6	0.8	175.4	Trace	213.3	520.0	74.8	1.09
7	1.0	290.1	Trace	258.1	550.7	65.5	1.09
8 <sup>e</sup>	—	235.0	Trace	244.9	547.2	70.0	1.06

<sup>a</sup> Additive concentration used for  $\text{CO}_2$  conversion. <sup>b</sup> Formation rate after 5 h of irradiation. <sup>c</sup> Selectivity toward CO evolution. <sup>d</sup> Ratio of consumed electrons to holes after 5 h of irradiation. <sup>e</sup> 0.5 M aqueous  $\text{NH}_3$  solution was used as the additive, instead of  $\text{NH}_4\text{HCO}_3$ .



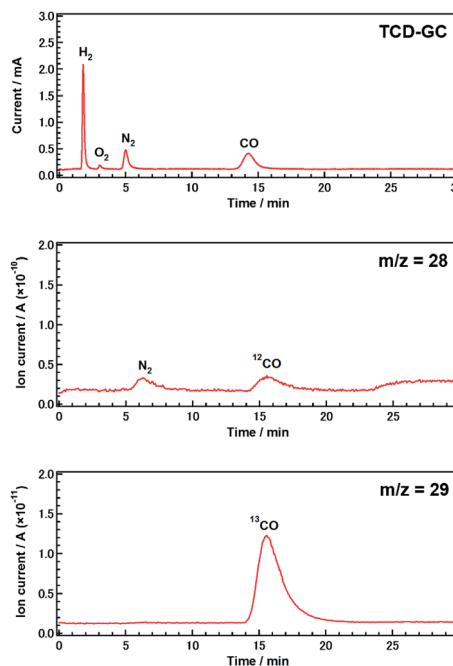


Fig. 2 Gas chromatogram and mass spectra ( $m/z = 28$  and  $29$ ) obtained during the photocatalytic conversion of  $^{13}\text{CO}_2$  using Ag-modified  $\text{Sr}_{1.6}\text{K}_{0.35}\text{Na}_{1.45}\text{Ta}_5\text{O}_{15}$ . Amount of catalyst:  $0.5\text{ g}$ ; cocatalyst loading:  $5.0\text{ wt\% Ag}$ ; light source:  $400\text{ W}$  high-pressure Hg lamp; water volume:  $1.0\text{ L}$ ;  $\text{CO}_2$  flow rate:  $30\text{ mL min}^{-1}$ ; additive:  $0.5\text{ M NH}_4\text{HCO}_3$ .

modified  $\text{Sr}_{1.6}\text{K}_{0.35}\text{Na}_{1.45}\text{Ta}_5\text{O}_{15}$  after  $0.5\text{ h}$  of photoirradiation. Gaseous samples were introduced into a mass spectrometer (MS) after separation by thermal conductivity detector-gas chromatography (TCD-GC). CO was observed in both the gas chromatogram and the mass spectra. The peak positions in the mass spectra were consistent with those in the chromatogram. The major product was  $^{13}\text{CO}$ , rather than  $^{12}\text{CO}$ . The presence of a small amount of  $^{12}\text{CO}$  may be due to the direct decomposition of  $\text{NH}_4\text{HCO}_3$  since the decomposition of  $\text{NH}_4\text{HCO}_3$  was observed in samples without a  $\text{CO}_2$  flow (Fig. S2D†). The amount of  $^{13}\text{CO}$  estimated by mass spectrometry was approximately equal to the amount of CO determined using a flame ionization detector (FID-GC) (Fig. S6†). These results demonstrate that CO was predominantly generated from  $\text{CO}_2$  introduced in the gas phase, rather than from other carbon resources.

The recycle test was also performed to confirm the stability and durability of our catalyst and system using the  $\text{Sr}_{1.6}\text{K}_{0.35}\text{Na}_{1.45}\text{Ta}_5\text{O}_{15}$  photocatalyst repeatedly for three times under the same conditions (Fig. S7†). In the second cycle, there is a slight loss by *ca.*  $10\%$  of CO evolution activity during  $5\text{ h}$  photo-irradiation as compared to the first run, however, the evolution of  $\text{H}_2$  showed no obvious changes. The slight loss of activity should be due to the change of Ag cocatalyst (Fig. S5†).<sup>29</sup> The photocatalytic activity of CO,  $\text{N}_2$ , and  $\text{H}_2$  were stabilized at *ca.*  $0.5$ ,  $0.19$  and  $0.07\text{ mmol h}^{-1}$ , respectively, during the second and third runs. The structure of catalyst itself was stable during the three cycles (Fig. S8†). These results suggested that the photocatalyst and the system exhibit favorable stability to form CO,  $\text{N}_2$ , and  $\text{H}_2$  during the photocatalytic conversion of  $\text{CO}_2$ .

Table 2 Photocatalytic conversion of  $\text{CO}_2$  over Ag-modified catalysts in aqueous  $\text{NH}_4\text{HCO}_3$  solution. Amount of catalyst:  $0.5\text{ g}$ ; cocatalyst loading:  $5.0\text{ wt\% Ag}$ ; light source:  $400\text{ W}$  high-pressure Hg lamp; water volume:  $0.95\text{ L}$ ;  $\text{CO}_2$  flow rate:  $30\text{ mL min}^{-1}$ ; additive:  $0.5\text{ M NH}_4\text{HCO}_3$

Entry	Catalyst	Formation rate <sup>a</sup> / $\mu\text{mol h}^{-1}$			
		$\text{H}_2$	$\text{N}_2$	CO	Selec. <sup>b</sup> (%)
1	$\text{ZnGa}_2\text{O}_4/\text{Ga}_2\text{O}_3$	125.2	191.4	532.0	80.9
2	$\text{ZnGa}_2\text{O}_4$	39.4	94.2	305.4	88.6
3	$\text{La}_2\text{Ti}_2\text{O}_7$	5.9	17.4	41.6	87.6
4	$\text{SrO/Ta}_2\text{O}_5$	2.71	11.5	42.9	94.1

<sup>a</sup> Formation rate after  $5\text{ h}$  of irradiation.  $\text{O}_2$  was not detected in any of the samples. <sup>b</sup> Selectivity toward CO evolution. <sup>c</sup> Ratio of consumed electrons to holes after  $5\text{ h}$  of irradiation.

To confirm the versatility of  $\text{NH}_4\text{HCO}_3$  as a general electron donor in photocatalytic reactions, we carried out the photocatalytic conversion of  $\text{CO}_2$  in aqueous  $\text{NH}_4\text{HCO}_3$  solution over 4 types of photocatalysts. All these photocatalysts have been already reported to show good activity and high selectivity toward CO evolution in the photocatalytic conversion of  $\text{CO}_2$  using  $\text{H}_2\text{O}$  as an electron donor.<sup>25,32-34</sup> As shown in Table 2, all the photocatalysts showed good activity for conversion of  $\text{CO}_2$  and high selectivity toward CO evolution. The activities of the photocatalysts were significantly increased in aqueous  $\text{NH}_4\text{HCO}_3$  solution, compared with their reported activities in pure  $\text{H}_2\text{O}$  or aqueous  $\text{NaHCO}_3$ .<sup>32-34</sup>  $\text{N}_2$  was detected as the only oxidation product and the  $\text{e}^-/\text{h}^+$  ratio was approximately equal to  $1.0$ . These results indicated that  $\text{NH}_3$  and/or  $\text{NH}_4^+$  was easily decomposed to  $\text{N}_2$  gas by the photocatalysts tested.

## Conclusions

We designed a highly efficient process for the photocatalytic conversion of  $\text{CO}_2$  to CO in aqueous  $\text{NH}_4\text{HCO}_3$  solution. The stoichiometric formation of CO,  $\text{H}_2$ , and  $\text{N}_2$  indicated that  $\text{NH}_3$  and/or  $\text{NH}_4^+$  were consumed as electron donors, instead of  $\text{H}_2\text{O}$ .  $\text{NH}_4\text{HCO}_3$  was determined to be an effective electron donor for the photocatalytic conversion of  $\text{CO}_2$ , whereby  $\text{CO}_2$  can be captured, stored, and efficiently converted into CO. This novel inorganic additive is suitable for use in carbon capture and utilization process. This new process is a promising way to control the conversion of  $\text{CO}_2$  to CO and efficiently produce  $\text{H}_2$  and CO.

## Acknowledgements

This study was partially supported by a Grant-in-Aid for Scientific Research on Innovative Areas “All Nippon Artificial Photosynthesis Project for Living Earth” (No. 2406) from the Ministry of Education, Culture, Sports, Science, and Technology (MEXT) of Japan, the Precursory Research for Embryonic Science and Technology (PRESTO), supported by the Japan Science and Technology Agency (JST), and the Program for Elements Strategy Initiative for Catalysts & Batteries (ESICB),

commissioned by the MEXT of Japan. Zeai Huang thanks the State Scholarship of China Scholarship Council, affiliated with the Ministry of Education of the P. R. China.

## Notes and references

- 1 S. N. Habisreutinger, L. Schmidt-Mende and J. K. Stolarczyk, *Angew. Chem., Int. Ed.*, 2013, **52**, 7372–7408.
- 2 G. Centi, E. A. Quadrelli and S. Perathoner, *Energy Environ. Sci.*, 2013, **6**, 1711–1731.
- 3 K. Teramura, S. Iguchi, Y. Mizuno, T. Shishido and T. Tanaka, *Angew. Chem.*, 2012, **124**, 8132–8135.
- 4 R. Kuriki, K. Sekizawa, O. Ishitani and K. Maeda, *Angew. Chem., Int. Ed.*, 2015, **54**, 2406–2409.
- 5 R. Kuriki, H. Matsunaga, T. Nakashima, K. Wada, A. Yamakata, O. Ishitani and K. Maeda, *J. Am. Chem. Soc.*, 2016, **138**, 5159–5170.
- 6 S. Navalón, A. Dhakshinamoorthy, M. Álvaro and H. García, *ChemSusChem*, 2013, **6**, 562–577.
- 7 X. Chang, T. Wang and J. Gong, *Energy Environ. Sci.*, 2016, **9**, 2177–2196.
- 8 G. Liu, S. Xie, Q. Zhang, Z. Tian and Y. Wang, *Chem. Commun.*, 2015, **51**, 13654–13657.
- 9 K. Iizuka, T. Wato, Y. Miseki, K. Saito and A. Kudo, *J. Am. Chem. Soc.*, 2011, **133**, 20863–20868.
- 10 M. Yamamoto, T. Yoshida, N. Yamamoto, T. Nomoto, Y. Yamamoto, S. Yagi and H. Yoshida, *J. Mater. Chem. A*, 2015, **3**, 16810–16816.
- 11 H. Yoshida, L. Zhang, M. Sato, T. Morikawa, T. Kajino, T. Sekito, S. Matsumoto and H. Hirata, *Catal. Today*, 2015, **251**, 132–139.
- 12 H. Nakanishi, K. Iizuka, T. Takayama, A. Iwase and A. Kudo, *ChemSusChem*, 2017, **10**, 112–118.
- 13 K. Hara, A. Kudo, T. Sakata and M. Watanabe, *J. Electrochem. Soc.*, 1995, **142**, L57–L59.
- 14 H. Yuzawa, T. Mori, H. Itoh and H. Yoshida, *J. Phys. Chem. C*, 2012, **116**, 4126–4136.
- 15 H. Wang, Y. Su, H. Zhao, H. Yu, S. Chen, Y. Zhang and X. Quan, *Environ. Sci. Technol.*, 2014, **48**, 11984–11990.
- 16 X. Zhu, S. R. Castleberry, M. A. Nanny and E. C. Butler, *Environ. Sci. Technol.*, 2005, **39**, 3784–3791.
- 17 S. Yamazoe, Y. Hitomi, T. Shishido and T. Tanaka, *Appl. Catal., B*, 2008, **82**, 67–76.
- 18 H. Kominami, H. Nishimune, Y. Ohta, Y. Arakawa and T. Inaba, *Appl. Catal., B*, 2012, **111**, 297–302.
- 19 B. T. Zhao, Y. X. Su, W. W. Tao, L. L. Li and Y. C. Peng, *Int. J. Greenhouse Gas Control*, 2012, **9**, 355–371.
- 20 X. Wang, W. Conway, D. Fernandes, G. Lawrence, R. Burns, G. Puxty and M. Maeder, *J. Phys. Chem. A*, 2011, **115**, 6405–6412.
- 21 S. F. Shen, Y. N. Yang and S. F. Ren, *Fluid Phase Equilib.*, 2014, **367**, 38–44.
- 22 H. Zhong, K. Fujii, Y. Nakano and F. Jin, *J. Phys. Chem. C*, 2015, **119**, 55–61.
- 23 B. Kumar, M. Llorente, J. Froehlich, T. Dang, A. Sathrum and C. P. Kubiak, *Annu. Rev. Phys. Chem.*, 2012, **63**, 541–569.
- 24 Y. Hori, A. Murata and R. Takahashi, *J. Chem. Soc., Faraday Trans. 1*, 1989, **85**, 2309–2326.
- 25 K. Teramura, Z. Wang, S. Hosokawa, Y. Sakata and T. Tanaka, *Chem.-Eur. J.*, 2014, **20**, 9906–9909.
- 26 E. E. Barton, D. M. Rampulla and A. B. Bocarsly, *J. Am. Chem. Soc.*, 2008, **130**, 6342–6344.
- 27 J. Boltersdorf, N. King and P. A. Maggard, *CrystEngComm*, 2015, **17**, 2225–2241.
- 28 Y. Ham, T. Hisatomi, Y. Goto, Y. Moriya, Y. Sakata, A. Yamakata, J. Kubota and K. Domen, *J. Mater. Chem. A*, 2016, **4**, 3027–3033.
- 29 Z. Huang, K. Teramura, S. Hosokawa and T. Tanaka, *Appl. Catal., B*, 2016, **199**, 272–281.
- 30 K. H. Lee, B. Lee, J. H. Lee, J. K. You, K. T. Park, I. H. Baek and N. H. Hur, *Int. J. Greenhouse Gas Control*, 2014, **29**, 256–262.
- 31 K. Teramura, K. Hori, Y. Terao, Z. Huang, S. Iguchi, Z. Wang, H. Asakura, S. Hosokawa and T. Tanaka, *J. Phys. Chem. C*, 2017, **121**, 8711–8721.
- 32 Z. Wang, K. Teramura, S. Hosokawa and T. Tanaka, *J. Mater. Chem. A*, 2015, **3**, 11313–11319.
- 33 Z. Wang, K. Teramura, S. Hosokawa and T. Tanaka, *Appl. Catal., B*, 2015, **163**, 241–247.
- 34 K. Teramura, H. Tatsumi, Z. Wang, S. Hosokawa and T. Tanaka, *Bull. Chem. Soc. Jpn.*, 2015, **88**, 431–437.

